

Synthesis and Ionic Conductivity of Supramolecular Layered Silicate Hybrids of Phosphotungstates and Poly(ethylene glycol) Dicarboxylates

Sang Kyeong Yun and Joachim Maier*

Max-Planck-Institut für Festkörperforschung,
Heisenbergstrasse 1, 70569 Stuttgart, Germany

Received July 22, 1998

Revised Manuscript Received February 17, 1999

Low-temperature synthetic techniques such as those usually denoted by the term *chimie douce* enable a certain nanoscale structural control and have been utilized to direct materials properties of solids such as catalytic activity and ionic conductivity.¹ By applying soft chemical synthetic methods, we were able to synthesize for the first time propylamine-functionalized ionic lamellar silicates, interlayered with $\text{PW}_{12}\text{O}_{40}^{3-}$ or poly(ethylene glycol) dicarboxylate, at ambient conditions. The present study demonstrates the structure-directing roles of $\text{H}_3\text{PW}_{12}\text{O}_{40}$ and poly(ethylene glycol) dicarboxylic acid in leading to layered supramolecular aminopolysilicates, as so far only amorphous materials have been reported by using HCl, HClO_4 , etc.^{2,3} In all cases we measured the conductivities by impedance spectroscopy, which we attributed to the protons in the networks. Electronic contributions seem to be insignificant in view of the chemistry and the low-frequency behavior of impedance spectra. Under a dry Ar atmosphere both series of layered silicate hybrids exhibited conductivities (σ) of up to 1.2×10^{-5} S/cm at 177 °C, mainly dependent on temperature (room temperature to 180 °C) and acid concentration. The comparatively higher proton conductivity gets lost in the amorphous state of a phosphotungstic acid derivative (σ drops by about 4 orders of magnitude).

Our approach is based on a one-step sol-gel synthesis of acid/base adducts between amine-functionalized organosilane and the inorganic or organic acids.⁴ In a typical synthesis, 91.6 mmol of (3-aminopropyl)triethoxysilane (APTEOS) was slowly added with good stirring to a clear solution of 5.0 g of phosphotungstic acid (PTA) dissolved in a water-ethanol mixture. A 3-fold molar excess of water, mixed with twice as much ethanol as APTEOS by volume, was used to fully hydrolyze APTEOS at room temperature.⁵ Within minutes after the delivery of basic APTEOS, white precipitates were obtained from the solution ([APTEOS]:[PTA]:[H₂O]:

* To whom correspondence should be addressed.

(1) (a) Judeinstein, P.; Sanchez, C. *J. Mater. Chem.* **1996**, *6*, 511–525. (b) Rouxel, J.; Tournoux, M. *Solid State Ionics* **1996**, *84*, 141–149 and references therein. (c) Rousset, A. *Solid State Ionics* **1996**, *84*, 293–301.

(2) Charbouillot, Y.; Ravaine, D.; Armand, M.; Poinsignon, C. *J. Non-Cryst. Solids* **1988**, *103*, 325–330.

(3) Armand, M. *Adv. Mater.* **1990**, *2*, 278–286 and references therein.

(4) Chemicals used: APTEOS (Alfa, 98%), PTA (Aldrich), PEGDA (Fluka, $M_n \sim 600$), ethanol (Carl Roth, 99.8%), and doubly distilled water, used for the preparation of all aqueous solutions.

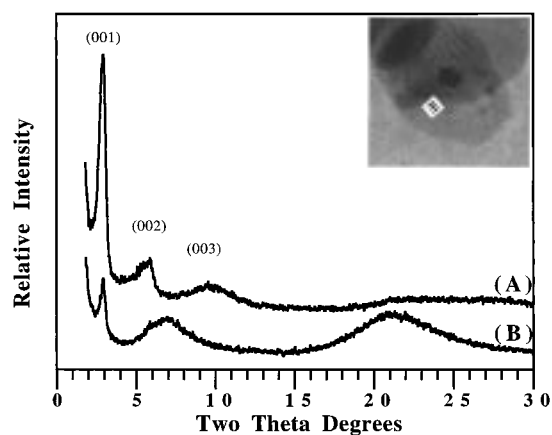


Figure 1. Representative powder XRD patterns of the prepared NHPTA and NHPEGDA samples. Diffraction patterns, obtained at room temperature with a Philips PW3710 diffractometer using $\text{Cu K}\alpha$ X-ray radiation, are shown for samples of (A) NHPTA-9 and (B) NHPEGDA-19 derivatives pretreated at 70 °C (10 h) and 100 °C (48 h), respectively. The inset is a high-resolution TEM picture of the NHPTA-9 sample, where the distances of the scale (which corresponds to the scale in Figure 2) are ~ 16 Å each.

$[\text{CH}_3\text{CH}_2\text{OH}] = 1.0:x/60$, $x = 1, 2, 4$, or $10:3.0:0.126$). After 30 min of further stirring at ambient conditions under a glass cover, the products were air-dried in a hood and then at 70 °C in an oven. Products of the general formula $[\text{SiO}_{1.5}(\text{CH}_2\text{CH}_2\text{CH}_2\text{NH}_2)_{1-3x/60}(\text{CH}_2\text{CH}_2\text{CH}_2\text{NH}_3^+)_{3x/60}][\text{PW}_{12}\text{O}_{40}^{3-}]_{x/60}$, where $x = 1, 2, 4$, or 10 , were obtained with the neutral amine ($1 - 3x/60$) to protonated amine ($3x/60$) ratios of $X = 19, 9, 4$, or 1 , respectively.⁵ Products are abbreviated hereafter as NHPTA- X .

Using poly(ethylene glycol) 600 dicarboxylic acid (PEGDA) at the same reaction conditions, optically transparent slurry products could be obtained. After 3 days of standing at room temperature, the initially viscous gels were further processed at 70 °C (1 week) and 120 °C (3 days), in a Petri dish covered with a glass plate, to solvent-free brittle thick films. The stoichiometric products of $[\text{SiO}_{1.5}(\text{CH}_2\text{CH}_2\text{CH}_2\text{NH}_2)_{1-2x/40}(\text{CH}_2\text{CH}_2\text{CH}_2\text{NH}_3^+)_{2x/40}][\text{O}_2\text{CCH}_2(\text{OCH}_2\text{CH}_2)_{\sim 10.6}\text{OCH}_2\text{CO}_2^-]_{x/40}$, where $x = 1, 2, 4$, or 10 , are designated hereafter as NHPEGDA-19, -9, -4, or -1, respectively, according to their neutral amine ($1 - 2x/40$) to protonated amine ($2x/40$) ratios as in NHPTA analogues.

As shown in Figure 1, up to 3 orders of (00 l) reflections were observed for the NHPTA-9 sample, indicative of a layered structural feature with a basal spacing of 30.0 Å. Though less featured, NHPTA-19 and -4 derivatives also exhibit similar patterns of (00 l) reflections with the same d spacing. In the case of NHPTA-1, however, there were only broad X-ray reflections cen-

(5) Stoichiometric sol-gel hydrolysis of APTEOS under an acidic condition is described as follows: $(\text{CH}_3\text{CH}_2\text{O})_3\text{SiCH}_2\text{CH}_2\text{CH}_2\text{NH}_2 + 1.5\text{H}_2\text{O} + n(\text{H}_m\text{X}^{m-}) \rightarrow 3\text{CH}_3\text{CH}_2\text{OH} + [\text{SiO}_{1.5}(\text{CH}_2\text{CH}_2\text{CH}_2\text{NH}_2)_{1-nm}(\text{CH}_2\text{CH}_2\text{CH}_2\text{NH}_3^+)_{nm}][n\text{X}^{m-}]$, where $1 - nm \geq 0$. ICP elemental analysis revealed the [W] to [Si] molar ratios of 0.21 (0.20), 0.39 (0.40), 0.77 (0.80), and 1.69 (2.00) for NHPTA-19, -9, -4, and -1, respectively (values in parentheses are the ones calculated based on the stoichiometric reactions).

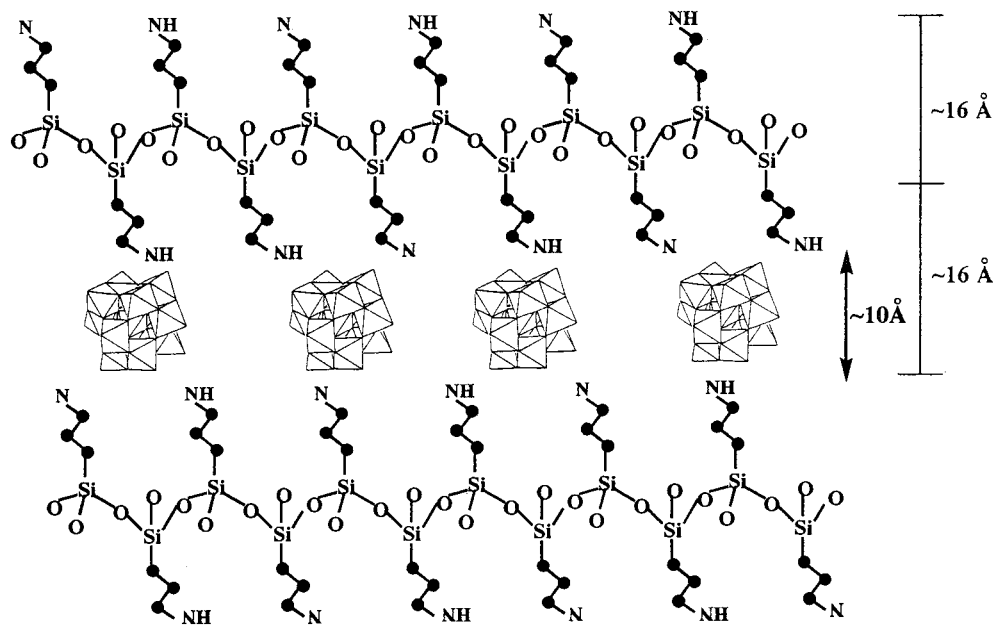


Figure 2. Proposed layered structure of the propylamine-functionalized zweier polysilicate interlayered with the Keggin-type phosphotungstate anion, $PW_{12}O_{40}^{3-}$. Alkyl carbon (closed circles) and amine groups (N) are shown with hydrogens omitted for clarity, except the acidic protons (NH). With respect to the scale confer the inset of Figure 1. (Note that not all of the elements are necessarily exactly in-plane in the projection.)

tered at ~ 11 Å, most probably due to an amorphous salt formation, as in other PTA-type amorphous salts.⁶

A layered structure was also indicated for all prepared NHPEGDA derivatives. Interestingly, a d spacing of 30.5 Å, almost the same as that of the layered NHPTA analogues (30.0 Å), was found at all four samples. An increase of the number of protonated amines, from NHPEGDA-19 to NHPEGDA-1, resulted in a reduced crystallinity of the layered feature, according to the relative intensity of their d_{001} reflections. All NHPEGDA derivatives showed broad X-ray reflections in the 5–9 and 17–26 2θ ranges, signifying less ordered layer stacking features, as is also reported for alkylamine-intercalated lamellar silicates.⁷ High-resolution transmission electron microscopy (HRTEM) showed that the observed asymmetry and broadness are not due to a second phase.

TEM studies⁸ of the NHPTA-9 sample revealed that the two alternating layers of polysilicate and Keggin ions of about 9–11 Å thickness are interlayered by about 5–7 Å spacings, which sum up to about 30–33 Å basal spacing (the inset in Figure 1). In addition, the observed selected area electron diffraction pattern was characteristic of a hexagonal array with $a = b = 5.4$ Å, indicating a six-membered zweier phyllosilicate-like structure.⁹ Tetragonal superlattice diffractions were also detected, which indicate the homogeneous distribution of the interlayer Keggin anions along the crystallographic ab direction. In fact, we could verify the

tetragonal arrangement of the Keggin ions, which appeared as dots in the TEM picture, on the external surface of a microcrystal. The framework structure of the Keggin-type PTA anion remained evidently unchanged during the preparation process, as verified by the presence of its authentic metal–oxygen vibrations¹⁰ in FTIR spectra.

Armand and co-workers^{2,3} reported on sol–gel formations of propylamine-functionalized amorphous polysilicates, the local microstructures of which are proposed to have a ladder-type puckered configuration. However, opposite to the synthesis described here, no extended anions have been used in refs 2 and 3. On the basis of our X-ray diffraction (XRD) and TEM results on the present materials, the nanoscale architecture shown in Figure 2 is proposed. Fully ionized PTA anions of the so-called Keggin structure with ~ 10 Å diameter¹⁰ are interlayered by two-dimensional propylamine-functionalized silicate sheets of ~ 20 Å thickness. Pseudotetrahedral $SiO_{1.5}(CH_2CH_2CH_2NH_2)$ units, protonated or neutral, are directioned up and down toward interlayer PTA anions. Corner-shared pseudotetrahedral silicates develop in the crystallographic ab direction with six-membered zweier phyllosilicate structure. Between the polysilicate layers the PTA units are tetragonally arranged and spaced in such a way that their negative charge is compensated by the protonated amine groups, which in turn are covalently grafted onto the silicate layers. The interlayer $PW_{12}O_{40}^{3-}$ ion will most likely have its C_2 axis of the oxygen framework orthogonal to the silicate layers to optimize hydrogen bonding interaction with the layer amine protons, as in the so-called layered double hydroxide (LDH) derivatives.¹¹ Different

(6) (a) McGarvey, G. B.; Taylor, N. J.; Moffat, J. B. *J. Mol. Catal.* **1993**, *80*, 59–73. (b) Brückman, K.; Tatibouët, J.-M.; Che, M.; Serwicka, E.; Haber, J. *J. Catal.* **1993**, *139*, 455–467. (c) Yun, S. K.; Pinnavaia, T. J. *Inorg. Chem.* **1996**, *35*, 6853–6860.

(7) Yanagisawa, T.; Shimizu, T.; Kuroda, K.; Kato, C. *Bull. Chem. Soc. Jpn.* **1990**, *63*, 988–992.

(8) High-resolution TEM studies were performed with a Philips CM 200 at 200 kV for samples prepared by dipping holey carbon-coated copper grids into a powder suspension in ethanol.

(9) Liebau, F. *Structural Chemistry of Silicates*; Springer-Verlag: Berlin/New York, 1985.

(10) Rocchiccioli-Deltcheff, C.; Fournier, M.; Franck, R.; Thouvenot, R. *Inorg. Chem.* **1983**, *22*, 207–216.

(11) (a) Kwon, T.; Pinnavaia, T. J. *Chem. Mater.* **1989**, *1*, 381–383. (b) Wang, J.; Tian, Y.; Wang, R.-C.; Clearfield, A. *Chem. Mater.* **1992**, *4*, 1276–1282.

from the LDH–Keggin ion intercalates, in our materials the positive charge (proton) exerted at the amine functional groups may be varied substantially. Because of this flexibility, the $\text{PW}_{12}\text{O}_{40}^{3-}$ ion can be incorporated between the layers, which is not possible at LDH systems because of their limited range of charge matching.¹¹ In the case of the highly protonated NHPTA-1, however, there is not enough room for the Keggin ion to form a layered structure in terms of charge compensation, which results in an amorphous phase.

In contrast to PTA, PEGDA has a conformational freedom along its flexible long alkyl chain. The fact that the observed interlayer distance of 10 Å is in close agreement with those (8.0–9.6 Å) of poly(ethylene oxide)-intercalated layered systems^{12,13} suggests two possibilities of the interlayer PEGDA configuration, that is, (i) multilayers of stacked planar conformation perpendicular to the layer *c* axis or (ii) helicoidal conformation of the oxyethylene units. Depending on the degree of the charge compensation between PEGDA anions and protonated amines, both interlayer configurations may be possible. This structural property of the PEGDA molecules may have played a decisive role in effectively structuring the hybrid layers of all NHPEGDA derivatives regardless of reactant composition.

Irrespective of the fact that the ionic conductivity is expected to increase with the number of available ions up to a protonation degree of about 50%, we observed the lowest σ values at NHPTA-1, which has the largest number of amino protons (Figure 3). Conductivity enhancement by more than ~4 orders of magnitude was observed for the NHPTA-19, -9, and -4 samples (5.4×10^{-6} – 9.2×10^{-7} S/cm at 170–176 °C, $E_a = 0.64$ – 0.79 eV) compared with NHPTA-1 (1.5×10^{-10} S/cm at 175 °C, $E_a = 0.75$ eV).¹⁴ Thus, it can be concluded that it is the layered feature which allows an easy and percolative proton hopping in contrast to the X-ray amorphous NHPTA-1.

On the other hand, more or less comparable proton conductivities were observed for all PEGDA derivatives: 1.5×10^{-6} – 1.2×10^{-5} at ~175 °C. In general, conductivity increased more or less proportionally to the number of amino protons available. However, as opposed to the NHPTA analogues which showed a monotonic increase in proton conductivity, NHPEGDA derivatives exhibited a non-Arrhenius behavior. Along with the site-to-site hopping through a matrix of continuous structural amines (which itself may lead to a complicated *T* dependence of the mobility), an additional conduction path through an oxygen channel of the interlayer PEGDA may be available for protons in the NHPEGDA intercalates, quite similar to that in many

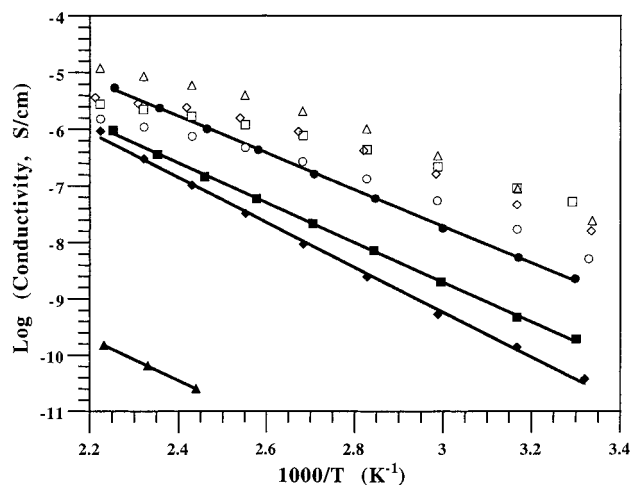


Figure 3. Temperature-dependent ionic conductivities of the NHPTA (closed symbols) and NHPEGDA (open symbols) derivatives: (i) rectangles, NHPTA- and NHPEGDA-19, (ii) circles, NHPTA- and NHPEGDA-9, (iii) diamonds, NHPTA- and NHPEGDA-4, and (iv) triangles, NHPTA- and NHPEGDA-1. In the case of NHPTA samples monotonic increases in the proton conductivity are shown curve-fitted into straight lines. Activation energies (E_a) derived from the slopes of the approximately linear lines are 0.70, 0.64, 0.79, and 0.75 eV for the NHPTA-19, -9, -4, and -1, respectively. E_a values for the NHPEGDA samples were calculated from the Vogel–Tammann–Fulcher (VTF) fit² employed for non-Arrhenius polymeric ion conductors: 0.087, 0.099, 0.080, and 0.093 eV for NHPEGDA-19, -9, -4, and -1, respectively.

oxygen-containing organic polymer systems of metal ion conductors.³ Hence, the lower activation energies observed in the NHPEGDA products compared to those of NHPTA analogues may be traced back to mechanistic differences.

The proposed anisotropic nature¹² of the observed proton conductivities could not be detected by impedance spectroscopy. For example, conductivities measured through the perpendicular and parallel directions on a pressed pellet of NHPTA-9 are 5.4×10^{-6} (at 170 °C) and 5.4×10^{-9} (at 42 °C) S/cm vs 6.9×10^{-6} (at 184 °C) and 5.3×10^{-9} (at 43 °C) S/cm, respectively. In the scanning electron microscope (SEM), particles of sub-micrometer-sized aggregates were found packed totally randomly in pressed-pellet samples used for the measurements, verifying that no preferential grain orientation was produced during the processing nor did it occur during the mechanical powder pressing. As a consequence, the impedance response is averaged over domains of different orientations and the anisotropy is lost in the overall measurements. This averaging also makes a standard interpretation of the conductivity speculative; however, it suggests much higher σ values if an efficient alignment could be achieved.

In summary, we have presented a soft chemical route to ionic lamellar structures of inorganic/organic hybrid silicates, which is distinguished from the surfactant-template¹⁵ or van der Waals interaction-based¹⁶ approach. Extended anions of the inorganic PTA and organic PEGDA are believed to act as a structure-

(12) Aranda, P.; Ruiz-Hitzky, E. *Chem. Mater.* **1992**, *4*, 1395–1403.

(13) (a) Ruiz-Hitzky, E.; Jimenez, R.; Casal, B.; Manriquez, V.; Ana, A. S.; Gonzalez, G. *Adv. Mater.* **1993**, *5*, 738–741. (b) Liu, Y.-J.; Schindler, J. L.; DeGroot, D. C.; Kannewurf, C. R.; Hirpo, W.; Kanatzidis, M. G. *Chem. Mater.* **1996**, *8*, 525–534.

(14) Conductivity measurements were carried out by the ac complex impedance method with a Solartron 1260 frequency response analyzer in the frequency range of 1.0 Hz to 30 MHz. Both sides of pressed-pellet samples were coated with platinum paste to provide better contacts with platinum electrodes. Measurements at various temperatures (room temperature to 180 °C), where no structural change was observed upon differential scanning calorimetry (DSC) experiments, were performed after 30 min of standing at each temperature (± 0.5 °C) under a dry Ar flow. Data collected during the cooling cycle were used to draw Cole–Cole plots for conductivity analysis.

(15) Kresge, C. T.; Leonowicz, M. E.; Roth, W. J.; Vartuli, J. C.; Beck, J. S. *Nature* **1992**, *359*, 710–712.

(16) Fukushima, Y.; Tani, M. *J. Chem. Soc., Chem. Commun.* **1995**, 241–242.

directing template in the formation of two-dimensional polysilicate upon the hydrolysis and polycondensation of APTEOS. A sensitive structural dependence of their proton conductivities was evident for the prepared amorphous and lamellar solids. Observed conductivity differences by about 4 orders of magnitude support the importance of the structural ordering, a finding which

(17) A preliminary study showed that prepared NHPTA and NHPEGDA derivatives exhibited appreciable reversible changes in the proton conductivity as a function of relative humidity. For example, 80% relative humidity even at 40 °C resulted in 2.01×10^{-6} (NHPTA-9) and 1.04×10^{-6} S/cm (NHPEGDA-1), compared with their dry Ar atmosphere conductivities of 5.42×10^{-9} and 8.94×10^{-8} S/cm, respectively.

may contribute to a further understanding and design of proton conductors.^{17,18}

Acknowledgment. S.K.Y. is thankful to the Max-Planck-Gesellschaft for a research scholarship. We also thank Dr. F. Phillipp and Ms. M. Kelsch from the Max-Planck-Institut for Metal Research for discussion and help in performing TEM studies.

CM9805166

(18) (a) Kreuer, K.-D.; Dippel, Th.; Hainovsky, N. G.; Maier, J. *Ber. Bunsen-Ges. Phys. Chem.* **1992**, *96*, 1736–1742. (b) Alberti, G.; Boccali, L.; Casciola, M.; Massinelli, L.; Montoneri, E. *Solid State Ionics* **1996**, *84*, 97–104. (c) Kreuer, K.-D. *Chem. Mater.* **1996**, *8*, 610–641.